Supplemental Experimental Procedures

Cell culture. IMR90 and WI38 human fibroblasts were cultured according to the ATCC in low oxygen (2%) and as previously described (Kennedy et al., 2011; Tu et al., 2011; Ye et al., 2007). Experiments were performed on IMR90 between population doubling #25-35. Addition of exogenous nucleosides (Sigma Aldrich, St. Louis, MO) was performed either at the start of infection or in established senescent cells as detailed in each experiment. Human melanoma cell lines were as previously described in ambient oxygen (21%) (Satyamoorthy et al., 1997), purchased from American Type Culture Collection (A375 cells), or kind gifts from Dr. Marianne B. Powell (Stanford University) (UACC-62 and UACC-903 cells). Normal human epidermal melanocytes were isolated from the epidermis of neonatal foreskin and cultured as previously described in ambient oxygen (21%) (Berking et al., 2004).

Plasmids and antibodies. pBABE-puro-H-RAS^{G12V}, pBABE-puro-BRAF^{V600E} and pBABE were obtained from Addgene. pGL2 was obtained from Promega (Madison, WI). pBABE-puro-RRM2, pGL2-RRM2, and pGL2-RRM2ΔE2F were generated using standard molecular cloning protocols, and details are available upon request. pLKO.1-shRRM2 plasmids were obtained from Open Biosystems. Human BRAF^{V600E} and NRAS^{Q61R} were subcloned into the pLU-EF1α-MCS-PGK-Blasticidin^{R} empty lentiviral plasmid by the protein expression facility at the Wistar Institute for their expression in normal human melanocytes. Details are available upon request.

The following antibodies were obtained from the indicated suppliers: goat anti-RRM2 (Santa Cruz Biotechnology, Santa Cruz, CA), rabbit anti-p21 (Abcam, Cambridge, MA), mouse anti-p53 (Calbiochem), mouse anti-p16 for western blotting (Santa Cruz Biotechnology), mouse anti-cyclin A (Novacastra Laboratories, Buffalo Grove, IL), rabbit

anti-Histone H3 (Millipore, Billerica, MA), mouse anti-RAS (BD Biosciences, San Jose, California), mouse anti-γH2AX (Millipore), rabbit anti-53BP1 (Bethyl, Montgomery, TX), rabbit anti-pS10H3 (Millipore), rabbit-anti E2F1 (Santa Cruz Biotechnology), mouse-anti BRAF (Santa Cruz Biotechnology), mouse anti-β-actin (Sigma), and mouse anti-BrdU FITC (BD Biosciences).

qRT-PCR and immunoblotting. qRT-PCR was performed using the iScript One-Step RT-PCR with SYBR Green kit (BioRad, Hercules, California). Primers for *RRM2* qRT-PCR were: Forward: 5'-TTTAGTGAGCTTAGCACAGCGGGA -3' and Reverse: 5'-AAATCTGCGTTGAAGCAGTGAGGC-3'. Primers for expression of the 5'UTR of *RRM2* were: Forward: 5'-AAAATCGCGCGCGGCCCCGC-3' and Reverse: GACCCCTCACTCCAGCAGC-3' and for ORF were: Forward: 5'TGGCAGACAGACTTATGCTGGA-3' and Reverse: 5'-GGACTTGACATCACTCCCATCC-3'. Primers for expression of E2F7 were: Forward: 5'-GGAAAGGCAACAGCAAACTCT-3' and Reverse: 5'-TGGGAGAGCACCAAGACTAGAAGA-3'. Primers for expression of E2F1 were: Forward: 3'-ATGAGACCTCACTGAATCTGACCACC-3' and Reverse: 3'-AGTCACAGTCGAAGAGGTCTCTG-3'. The expression of β-2-microglobulin mRNA expression was used to normalize *RRM2* mRNA expression. Immunoblotting was performed using the antibodies indicated above.

Luciferase promoter activity and mutagenesis analysis. A fragment of the proximal promoter of the human *RRM2* gene (-1071 to +76) and the mutant RRM2 (with the E2F binding site deleted) were generated by PCR and cloned into the pGL2 basic luciferase reporter plasmid (Promega) using standard molecular cloning protocols (details are

available upon request). Plasmids were transfected using the Amaxa electroporation system on day 2 as described previously (Tu et al., 2011).

Human nevi and melanoma specimens, immunohistochemical staining and scoring, and mutational analysis. Human nevi and melanoma tissues used in immunohistochemical staining were obtained from Fox Chase Cancer Center, and their pathological status was verified by Dr. Hong Wu, a board-certified pathologist. Use of these human specimens was approved by the Institutional Review Board. The expression of RRM2 was detected using avidin–biotin–peroxidase methods and as previously described (Bitler et al., 2011). Briefly, tissue sections were subjected to antigen retrieval by steaming in 0.01 mol/L of sodium citrate buffer (pH 6.0) for 30 minutes. After quenching endogenous peroxidase activity with 3% hydrogen peroxide and blocking nonspecific protein binding with 1% bovine serum albumin, sections were incubated overnight with an goat anti-RRM2 antibody (Santa Cruz Biotechnology; 1:500) at 4°C, followed by biotinylated rabbit anti-goat IgG (Dako, Carpinteria, CA; 1:100) for 1 hour, detecting the antibody complexes with the labeled streptavidin-biotin system (Dako), and visualizing them with the chromogen 3,30- diaminobenzidine. Sections were lightly counterstained with hematoxylin. In addition, anti-Ki67 (Dako, 1:100) and p16 (kind gift from Dr. Greg Enders, Fox Chase Cancer Center) antibodies were used on consecutive sections as previously described (Li et al., 2010). The expression of RRM2 was scored based on a histological score as previously described (McCarty et al., 1985; McCarty et al., 1986). To examine BRAF and NRAS mutation status, tissues were macrodissected manually under a microscope to select areas in which tumor cells dominated over stromal cells. PCR was performed to amplify BRAF exon 15 and NRAS exon 2 and 3. Primer sets and protocols for PCR were as previously described (Landi et al., 2006; Ohashi et al., 2012). PCR products were purified with the QIAquick Gel

Extraction Kit (Qiagen) and then sequenced to determine mutation status.

Colony formation assay and growth curve analysis. For colony formation, equal number of cells (3,000 cells/well) was inoculated in 6-well plates and cultured for additional 2 weeks. The colony formation was visualized by staining the plates with 0.05% crystal violet as previously described (Tu et al., 2011). Growth curves were generated by plating an equal amount of cells (20,000 cells/well) and counting the cell number at the indicated time points.

Data Sets, Survival and Statistical Analysis. The gene expression microarray data consisted of malignant melanoma patients were obtained from Gene Expression Omnibus (GEO accession number GSE8401) (Xu et al., 2008). 50 melanoma patients with oncogenic mutations in either BRAF or NRAS were selected for analysis. Raw data generated from Affymetrix Human Genome U133A Array Chip were normalized, background-corrected, and summarized by the robust multi-array (RMA) procedure (Irizarry et al., 2003) using the R package “affy”. The samples were divided into “high” vs. “low” based on the gene expression level using a ~70% cutoff. Survival was defined as the time elapsed from resection to the last clinical visit or death. Kaplan-Meier estimates of survival plots were generated, and comparisons between groups were made using the Mantel-Haenszel test. The χ^2 test was used to analyze the relationship between categorical variables. For all statistical analyzes, the level of significance was set at 0.05.

Supplemental Figure Legends

Figure S1. Addition of exogenous nucleosides is not sufficient to overcome the doxorubicin or etoposide-induced senescence-associated cell growth arrest; related to Figure 1.

(A) Schematic of experimental design and reference time frame unless otherwise specified.

(B) IMR90 cells were treated with 100 ng/ml doxorubicin and supplemented with or without indicated concentration of exogenous nucleosides. Seven days later, cells were stained for SA-β-gal activity.

(C) Quantification of SA-β-gal activity in (B). 200 cells from each of the indicated groups were examined for SA-β-gal activity.

(D) Same as (B), but an equal number of cells was inoculated into 6-well plates and after an additional 2 weeks in culture, the plates were stained with 0.05% crystal violet in PBS to visualize colony formation.

(E) Same as (D) but an equal number of cells were inoculated into 6-well plates counted four days later.

(F) IMR90 cells were treated with 10μM etoposide and supplemented with or without indicated concentration of exogenous nucleosides. Seven days later, cells were stained for SA-β-gal activity.

(G) Quantification of SA-β-gal activity in (F). 200 cells from each of the indicated groups were examined for SA-β-gal activity.

(H) Same as (F) but an equal number of cells was inoculated into 6-well plates and after an additional 2 weeks in culture, the plates were stained with 0.05% crystal violet in PBS to visualize colony formation.

(I) Same as (H) but an equal number of cells were inoculated into 6-well plates counted four days later.

Figure S2. Addition of exogenous nucleosides is sufficient to overcome the oncogene-induced senescence-associated cell growth arrest; related to Figure 2.

(A) IMR90 cells were infected with control or RAS-encoding retrovirus. On day 6, the cells were labeled with BrdU for 1 hour, and the incorporated BrdU was visualized by immunofluorescence staining. DAPI counterstaining was used to visualize nuclei.

(B) Quantification of (A). At least 200 cells from each of the indicated groups were examined for BrdU incorporation. Mean of four independent experiments with SEM.

(C) Same as (A) but an equal number of cells (3000 cells/well) were inoculated in 6-well plates with or without addition of exogenous nucleosides, and the number of cells was counted at the indicated time points. Mean of three independent experiments with SEM. *$p<0.05$

(D) Same as (C) but examined for RAS expression by immunoblotting. β-actin was used as a loading control.

(E) IMR90 cells were infected with control or RAS-encoding retrovirus. On day 12, cells were supplemented with or without 250 nM exogenous nucleosides (NS) and were stained for SA-β-gal activity after 2 weeks of additional culture.

(F) Quantification of (E). At least 200 cells were examined for SA-β-gal activity. Mean of three independent experiments with SEM.

(G) Same as (E) but equal number of cells were inoculated and counted after 2 weeks of additional culture. Mean of three independent experiments with SEM.

(H) WI38 primary human fibroblasts were infected with control or RAS-encoding retrovirus. On day 6, the cells were labeled with BrdU for 1 hour, and the incorporated

BrdU was visualized by immunofluorescence staining. DAPI counterstaining was used to visualize nuclei.

(I) Quantification of (H). At least 200 cells were examined for BrdU incorporation. Mean of three independent experiments with SEM.

(J) WI38 cells were infected with RAS-encoding retrovirus and senesced for 6 days. On day 6, the RAS-infected cells were seeded in 6-well plates and supplemented with or without 250 nM nucleosides (NS). The number of cells was counted after 2 weeks of additional culture.

Figure S3. Downregulation of RRM2 occurs prior to the OIS-associated cell cycle exit; related to Figure 3.

(A) IMR90 cells were infected with control or RAS-encoding retrovirus, and the cell cycle profile was determined using propidium iodide and flow cytometry at the indicated time points.

(B) Same as (A) but examined for RRM2, pS10H3, p16 and p21 protein expression by immunoblotting at the indicated time points. β-actin was used as a loading control.

(C) IMR90 cells were infected with control or RAS-encoding retrovirus. On day 2, the cells were labeled with BrdU for 1 hour and examined for BrdU incorporation by immunofluorescence staining. DAPI counterstaining was used to visualize nuclei.

(D) Quantification of (C). 200 cells from each of the indicated groups were examined for BrdU incorporation. Mean of three independent experiments with SEM. Note that no statistical significance was observed between control and RAS-expressing cells.

(E) Same as (C) but examined for RAS and cyclin A protein expression by immunoblotting. β-actin was used as a loading control.

(F) Schematic of DNA combing analysis protocol.

(G) Schematic and representative examples of elongating, terminated, and newly fired replication forks.

Figure S4. RRM2 downregulation is not due to the senescence-associated cell cycle exit and is not merely a consequence of the DNA damage response; related to Figure 4.

(A) IMR90 cells were infected with control or RAS-encoding retrovirus, and the expression of RRM1 and p53R2 was determined in drug-selected cells by qRT-PCR at day 1.

(B) IMR90 cells were infected with a lentivirus encoding shRRM2 (#1) that effectively knocks down RRM2 expression (e.g., Figure S4A) or control. The expression of RRM2 in drug-selected cells was determined by immunofluorescence staining. The arrow points to an example of RRM2 positively stained cells. Note that knockdown of RRM2 significantly decreased the RRM2 staining, suggesting that the staining signal observed in controls is specific.

(C) IMR90 cells were irradiated with 2Gy gamma radiation (IR), and RRM2 and γH2AX protein expression was examined by immunoblotting. β-actin was used as a loading control.

(D) Control proliferating cells were electroporated with a luciferase reporter driven by a wild-type human proximal *RRM2* gene promoter (-1071 to +76) or a vector control using Amaxa as described in Methods. A luminescent β-galactosidase reporter was used as an internal control to normalize the transfection efficacy. Mean of three independent experiments with SEM.

Figure S5. Knockdown of RRM2 in primary human fibroblasts induces senescence; related to Figure 5.

(A) IMR90 cells were infected with two individual lentivirus encoding the indicated shRRM2 or control. RRM2 and β-actin protein expression in the drug-selected cells was determined by immunoblotting.

(B) IMR90 cells were infected with a lentivirus encoding shRRM2 (#1) or control. On day 2, dNTP concentrations were determined in drug-selected cells.

(C) Same as (A) but the DNA replication dynamics in the drug-selected cells were examined using the DNA combing technique at day 2. *$p<0.05$ control vs. shRRM2 #1 or shRRM2 #2

(D) Same as (A) but formation of 53BP1 and γH2AX foci was determined by immunofluorescence staining on day 6.

(E) Quantification of (F). 200 cells from each of the indicated groups were examined for formation of the indicated foci. Mean of three independent experiments with SEM. *$p<0.001$ compared with controls.

(F) Same as (D) but examined for γH2AX and p53 protein expression by immunoblotting. β-actin was used as a loading control.

(G) Same as (D) but staining for SA-β-gal activity.

(H) Quantification of (G). 200 cells from each of the indicated groups were examined for SA-β-gal activity. Mean of three independent experiments with SEM. *$p<0.001$

(I) Same as (D) but examined for expression of cyclin A and pS10H3 by immunoblotting. β-actin was used as a loading control

(J) Same as (A) but the cells were labeled with BrdU for 1 hour, and the incorporated BrdU was visualized by immunofluorescence staining. DAPI counterstaining was used to visualize nuclei.

(K) Quantification of (J). 200 cells from each of the indicated groups were examined for BrdU incorporation, and the relative percentage of BrdU positive cells was calculated against vector controls. Mean of three independent experiments with SEM. *p<0.001

(L) Same as (A) but equal number of the indicated cells (3000 cells/well) were seeded in 6-well plates. After 2 weeks of additional culture, the plates were stained with 0.05% crystal violet in PBS to visualize colony formation. Shown are representative images from three independent experiments.

Figure S6. RRM2 is downregulated in melanocytes expressing mutant NRAS, and knockdown of RRM2 drives senescence of human melanoma cells; related to Figure 7.

(A) Melanocytes were infected with a lentivirus encoding control or $NRAS^{Q61R}$. Twenty-one days after infection, cells were examined for expression of RAS and RRM2 by immunoblotting. β-actin was used as a loading control.

(B) Same as (A) but examined for SA-β-gal activity.

(C) Quantification of (B). 200 cells from each of the indicated groups were examined for SA-β-gal staining. Mean of two independent experiments with SEM. *p<0.005

(D) Same as (A) but cells were supplemented with or without 50 nM exogenous nucleosides. Twenty-one days after infection, cells were stained for SA-β-gal activity.

(E) Quantification of (D). 200 cells from each of the indicated groups were examined for SA-β-gal staining. Mean of three independent experiments with SEM.

(F) Same as (D) but cells were examined for expression of pS10H3, p21, and γH2AX by immunoblotting. β-actin was used as a loading control.

(G) Cells were co-infected with retrovirus encoding control or RAS together with or without different amounts of RRM2. Drug-selected cells were examined for expression of RRM2 and RAS by immunoblotting. β-actin was used as a loading control.

(H) Same as (G) but cells were examined for γH2AX foci formation by immunofluorescence. Mean of three independent experiments with SEM.

(I-J) Quantification of p16 (I) and Ki67 (J) expression using the histological score in human benign nevi (n=5) and melanoma tissue specimens (n=7) harboring oncogenic BRAF or NRAS.

(K) A high level of RRM1 expression does not correlate with shorter overall survival in human melanoma patients with oncogenic BRAF or NRAS. The univariate overall survival curve (Kaplan-Meier method) for melanoma patients with oncogenic BRAF or NRAS (n=50) with high- or low- RRM1 expression as detailed in methods.

(L) WM164 human melanoma cells were infected with a lentivirus encoding control or two individual shRRM2s and the infected cells were selected with 1 μg/ml puromycin. On day 6, RRM2, pS10H3 and γH2AX protein expression in drug-selected cells was analyzed by immunoblotting. β-actin was used as a loading control.

(M) Same as (L) but an equal number of cells (3000) were seeded, and the total cell number was counted at the indicated time points. *$p<0.001$

(N) Same as (L) but after an additional 2 weeks in culture, the plates were stained with 0.05% crystal violet in PBS to visualize colony formation. Shown are representative images of two independent experiments.

(O) Same as (L) but stained for SA-β-gal activity.

(P) Quantification of (J). 200 cells from each of the indicated groups were examined for SA-β-gal staining. Mean of two independent experiments with SEM. *$p<0.05$

Cited References:

Berking, C., Takemoto, R., Satyamoorthy, K., Shirakawa, T., Eskandarpour, M., Hansson, J., VanBelle, P.A., Elder, D.E., and Herlyn, M. (2004). Induction of melanoma phenotypes in human skin by growth factors and ultraviolet B. Cancer Res *64*, 807-811.

Bitler, B.G., Nicodemus, J.P., Li, H., Cai, Q., Wu, H., Hua, X., Li, T., Birrer, M.J., Godwin, A.K., Cairns, P.*, et al.* (2011). Wnt5a suppresses epithelial ovarian cancer by promoting cellular senescence. Cancer Res *71*, 6184-6194.

Irizarry, R.A., Bolstad, B.M., Collin, F., Cope, L.M., Hobbs, B., and Speed, T.P. (2003). Summaries of Affymetrix GeneChip probe level data. Nucleic Acids Res *31*, e15.

Kennedy, A.L., Morton, J.P., Manoharan, I., Nelson, D.M., Jamieson, N.B., Pawlikowski, J.S., McBryan, T., Doyle, B., McKay, C., Oien, K.A.*, et al.* (2011). Activation of the PIK3CA/AKT pathway suppresses senescence induced by an activated RAS oncogene to promote tumorigenesis. Mol Cell *42*, 36-49.

Landi, M.T., Bauer, J., Pfeiffer, R.M., Elder, D.E., Hulley, B., Minghetti, P., Calista, D., Kanetsky, P.A., Pinkel, D., and Bastian, B.C. (2006). MC1R germline variants confer risk for BRAF-mutant melanoma. Science *313*, 521-522.

Li, H., Cai, Q., Godwin, A.K., and Zhang, R. (2010). Enhancer of zeste homolog 2 promotes the proliferation and invasion of epithelial ovarian cancer cells. Mol Cancer Res *8*, 1610-1618.

McCarty, K.S., Jr., Miller, L.S., Cox, E.B., Konrath, J., and McCarty, K.S., Sr. (1985). Estrogen receptor analyses. Correlation of biochemical and immunohistochemical methods using monoclonal antireceptor antibodies. Arch Pathol Lab Med *109*, 716-721.

McCarty, K.S., Jr., Szabo, E., Flowers, J.L., Cox, E.B., Leight, G.S., Miller, L., Konrath, J., Soper, J.T., Budwit, D.A., Creasman, W.T.*, et al.* (1986). Use of a monoclonal anti-estrogen receptor antibody in the immunohistochemical evaluation of human tumors. Cancer Res *46*, 4244s-4248s.

Ohashi, K., Sequist, L.V., Arcila, M.E., Moran, T., Chmielecki, J., Lin, Y.L., Pan, Y., Wang, L., de Stanchina, E., Shien, K.*, et al.* (2012). Lung cancers with acquired resistance to EGFR inhibitors occasionally harbor BRAF gene mutations but lack mutations in KRAS, NRAS, or MEK1. Proc Natl Acad Sci U S A *109*, E2127-2133.

Satyamoorthy, K., DeJesus, E., Linnenbach, A.J., Kraj, B., Kornreich, D.L., Rendle, S., Elder, D.E., and Herlyn, M. (1997). Melanoma cell lines from different stages of progression and their biological and molecular analyses. Melanoma Res *7 Suppl 2*, S35-42.

Tu, Z., Aird, K.M., Bitler, B.G., Nicodemus, J.P., Beeharry, N., Zia, B., Yen, T.J., and Zhang, R. (2011). Oncogenic Ras regulates BRIP1 expression to induce dissociation of BRCA1 from chromatin, inhibit DNA repair, and promote senescence. Dev Cell *21*, 1-15.

Xu, L., Shen, S.S., Hoshida, Y., Subramanian, A., Ross, K., Brunet, J.P., Wagner, S.N., Ramaswamy, S., Mesirov, J.P., and Hynes, R.O. (2008). Gene expression changes in

an animal melanoma model correlate with aggressiveness of human melanoma metastases. Mol Cancer Res *6*, 760-769.

Ye, X., Zerlanko, B., Kennedy, A., Banumathy, G., Zhang, R., and Adams, P.D. (2007). Downregulation of Wnt signaling is a trigger for formation of facultative heterochromatin and onset of cell senescence in primary human cells. Mol Cell *27*, 183-196.

Supplemental Figure 1

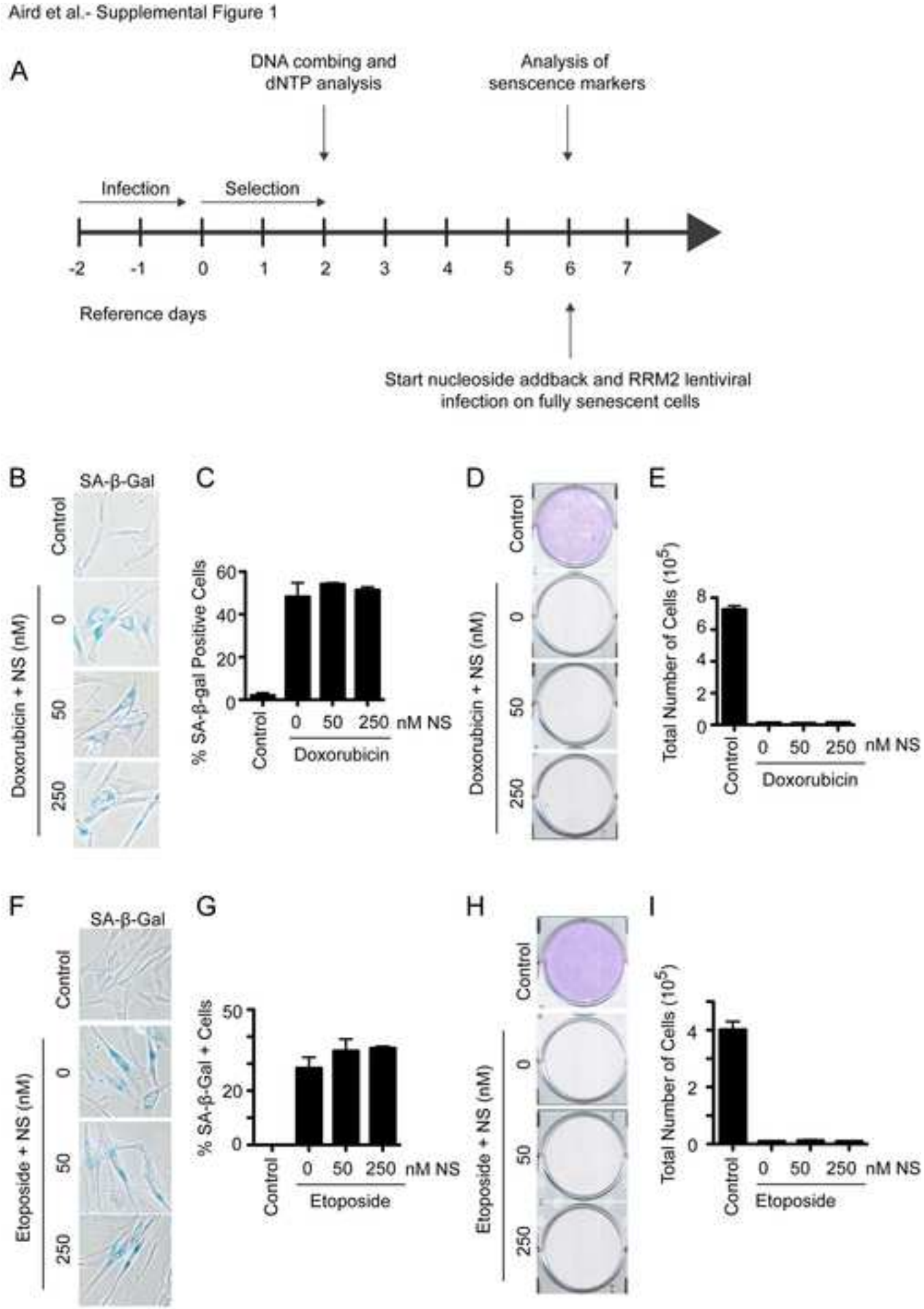

Supplemental Figure 2

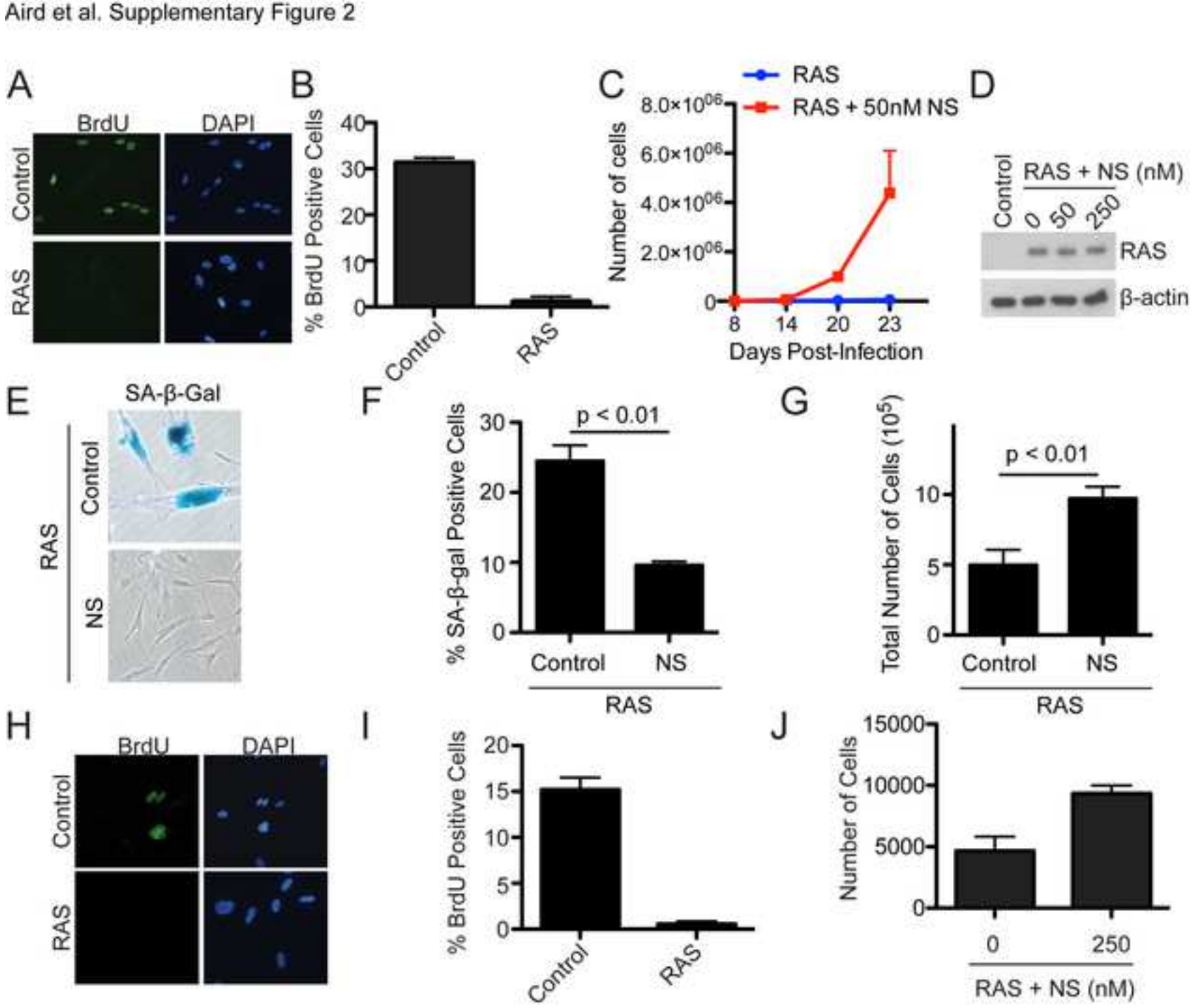

Supplemental Figure 3

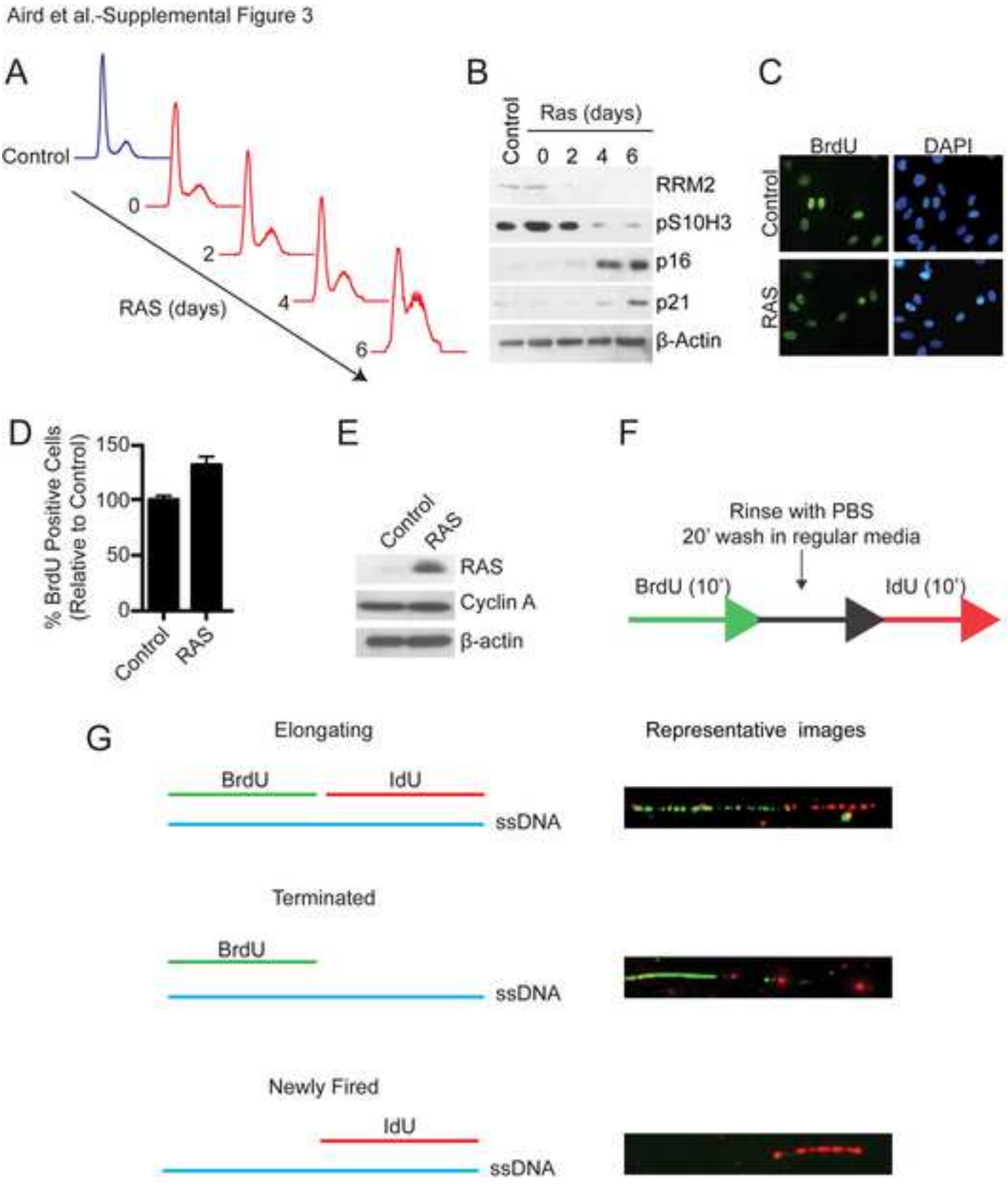

Aird et al.- Supplemental Figure 4

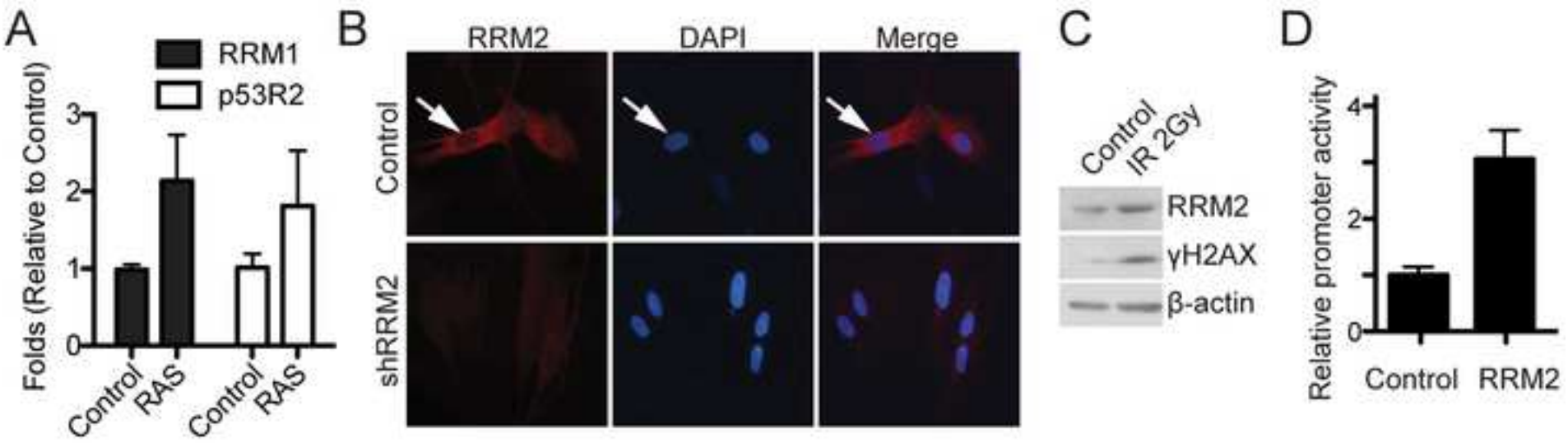

Supplemental Figure 5

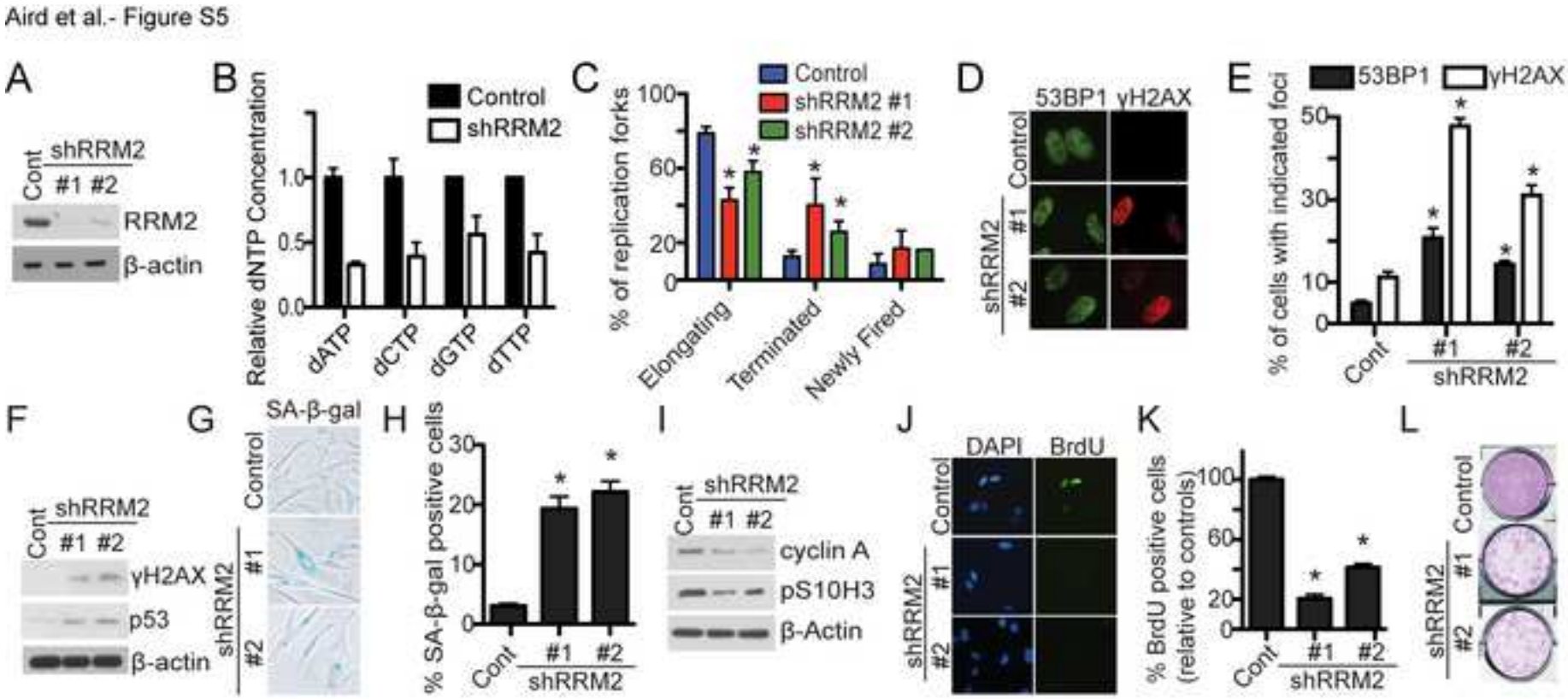

Supplemental Figure 6